PERGAMON

Vision Research 41 (2001) 541–548

Vision Research

www.elsevier.com/locate/visres

Rapid communication

Study of colour discrimination with comb-filtered spectra

Valérie Bonnardel [a,*], Eva M. Valero [b]

[a] *Department of Physiology, Downing Street, University of Cambridge, Cambridge CB2 3EG, UK*
[b] *Departamento de Optica, Falcultad de Ciencias, Universidad de Granada, 18071 Granada, Spain*

Received 14 April 2000; received in revised form 20 September 2000

Abstract

Techniques that involve the use of comb-filtered spectra to study human colour vision have been developed in previous work (Bonnardel, V., Bellemare, H., Mollon, J.D., 1996. Measurements of human sensitivity to comb-filtered spectra, Vision Research 36, 2713–2720; Bonnardel, V., Ruderman D.L., Barlow, H.B., 1997. A fast determination of the Spectral Modulation Sensitivity Function: a comparison between trichromats and deuteranopes. In: C.R. Cavonius (ed.), Color vision deficiencies XIII. Dordrecht: Kluver 415–424). These techniques are applied in the present study to measure colour discrimination among deuteranomalous observers and normal trichromats, with the aim of determining the spectral position of the anomalous cone fundamentals. Results show that comb-filtered spectra are useful in determining the extent to which variability in colour discrimination among anomalous and normal trichromatic colour observers is accounted for by the spectral properties of photoreceptors.

Keywords: Colour discrimination; Anomalous trichromacy; Comb-filtered spectra; Individual differences

1. Introduction

Comb-filtered spectra are colour stimuli whose spectral energy is modulated sinusoidally as a function of wavelength (Barlow, 1982). Their parameters include comb frequency, which is defined as the number of cycles per 300 nm over the range 400–700 nm, phase, amplitude of modulation and mean luminance. For a given comb frequency at a constant level of modulation, the set of chromaticity co-ordinates of comb-filtered spectra produced when phase varies from 0 to 360 deg describes an ellipse around the neutral point (unmodulated spectrum) (Brill & Benzschawel, 1985; Bonnardel, Bellemare, & Mollon, 1996). By varying phase, one can thus probe colour discrimination in all chromatic directions (see Fig. 1). By varying amplitude of modulation, one can vary stimulus saturation along an axis that joins an unsaturated neutral point with an amplitude of zero to a most-saturated point that corresponds to a fully modulated comb-filtered spectrum with an amplitude of one. By varying comb frequency, one can generate different ellipses in a chromaticity diagram by varying phase and holding amplitude constant. It is thus possible to present a stimulus of a given chromaticity in an infinite number of ways using comb-filtered spectra, by properly trading off their frequency, phase and amplitude.

An observer's cone fundamentals determine which comb-filtered spectra are metameric for that individual. If, when calculating chromaticity coordinates, one chooses the correct set of fundamentals for a given observer, then discrimination ellipses derived for two sets of comb-filtered spectra that differ in frequency will have the same size, position, and orientation in a chromaticity diagram. This is because discrimination thresholds at two different comb frequencies and generally different phases must be identical if they lie in the same direction away from the unsaturated neutral point. Hence the ellipses traced out for the two comb frequencies must be the same. We have used this principle in reverse: by finding the fundamentals that make

* Corresponding author.
E-mail address: vb10006@cus.cam.ac.uk (V. Bonnardel).

0042-6989/01/$ - see front matter
PII: S0042-6989(00)00278-9

discrimination ellipses at two comb frequencies most similar, we determined the spectral position of the cone fundamentals. This has been done for the anomalous cone fundamental of four deuteranomalous observers under large field or small field conditions. Two normal trichromats have acted as controls.

2. Method

2.1. Comb-filtered spectra

The comb-filtered spectra are generated by a stimulator that has been fully described elsewhere (Bonnardel et al., 1996; Bonnardel, 1998). The apparatus uses an interference wedge to spread the spectrum of the light from a short-arc xenon bulb of 150 W. The resulting light provides a spatially continuous linear spectrum from 400 to 700 nm in the plane of a liquid crystal display (LCD). The LCD is modulated sinusoidally (Fig. 2A) in space to provide a corresponding wavelength modulation in the spectral power distribution $E(\lambda)$ provided by the apparatus to the observer (Fig. 2B):

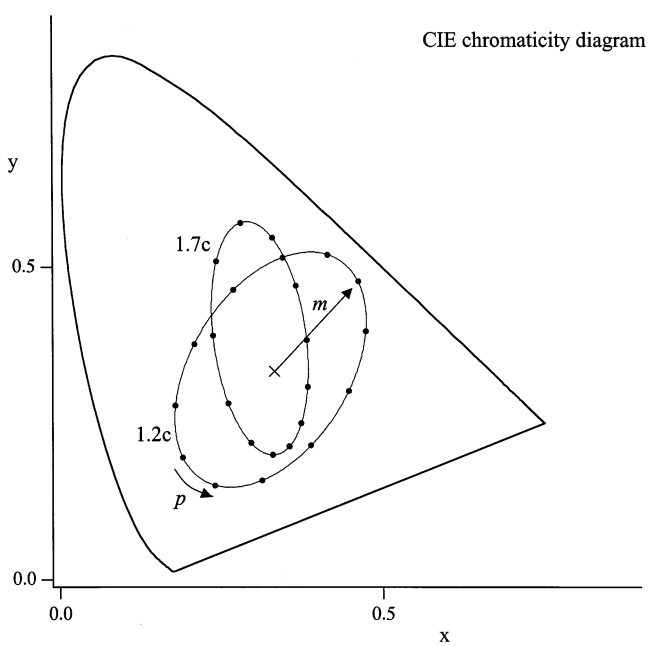

Fig. 1. Chromaticities of theoretical comb-filtered spectra were computed for 2 comb frequencies for 30 deg steps at a maximal level of modulation. The chromaticities are fit perfectly by an ellipsoidal contour. Shifting phase (p) changes direction in the chromaticity diagram, measured with respect to the chromaticity of the neutral, unmodulated spectrum (cross), while altering amplitude (m) allows saturation to vary from the unmodulated spectrum to the ellipsoidal contour, which corresponds to the most saturated stimuli. The locus of the unmodulated spectrum (here $x = 0.33$; $y = 0.33$) lies inside the ellipsoidal contour but does not correspond to a particular point of the ellipse (centre or focus).

$$E(\lambda) = E_0(\lambda)[1 + m \sin(fp(\lambda) + p_0)] \quad (1)$$

in which $E_0(\lambda)$ is the spectral power distribution of the unmodulated spectrum, m is the amplitude of the modulation, f is the comb frequency expressed in cycles per 300 nm (a unit hereinafter denoted c), p_0 is the phase, and $p(\lambda) = 1.2\lambda - 480$ scales the spectral interval to match the interval 0–360 deg. In these experiments, comb-filtered spectra of frequency either 1.2 or 1.7 c were used. These two comb frequencies were chosen from the interval of optimal sensitivity measured among normal trichromats in earlier work (Bonnardel et al., 1996; Bonnardel, Ruderman, & Barlow, 1997), but differed sufficiently to generate noticeable differences in chromaticities (Fig. 2C).

2.2. Procedure

Observers viewed the stimuli monocularly and used a chin rest. The stimulus comprised either an annulus of outer radius 8.5 deg visual angle with the central 4 deg occluded (large field condition) or a 2 deg spot displayed on a background of similar luminance (small field condition). The LCD was used to vary the luminance of the test randomly between 5.5 and 10.4 cd/m^2 with a mean of 8 cd/m^2, in order to ensure that responses were based on colour rather than luminance cues.

The observers indicated which stimulus differed from two others in a three temporal alternative forced-choice task. A staircase procedure was used to determine the modulation required by an observer to distinguish the single test with the modulated spectrum from the two reference stimuli with unmodulated spectra. The mean value of the last four staircase reversals, among a total of ten, was taken as threshold for that staircase. Four staircases were randomly interleaved per measurement. The large field condition with the annulus was used in the first set of measurements. Stimulus duration was 1 s. Three deuteranomalous observers (CS, AH and AWH) and one normal trichromat (EV) were tested in these conditions. In a second set of measurements, stimulus duration was reduced to 0.5 s, to shorten the duration of the experiment. One deuteranomalous observer (BR) was tested in the small field condition with the 2 deg spot, while one normal trichromat (VB) was tested in both small and large field conditions.

2.3. Computation of chromaticity coordinates

Stimulus spectral power distributions were measured using an Ocean Optics S2000 spectrometer that had previously been calibrated using a luminance standard in our laboratory. Chromaticity coordinates of comb-filtered spectra were computed in the small field condition using the CIE 1931 standard observer colour

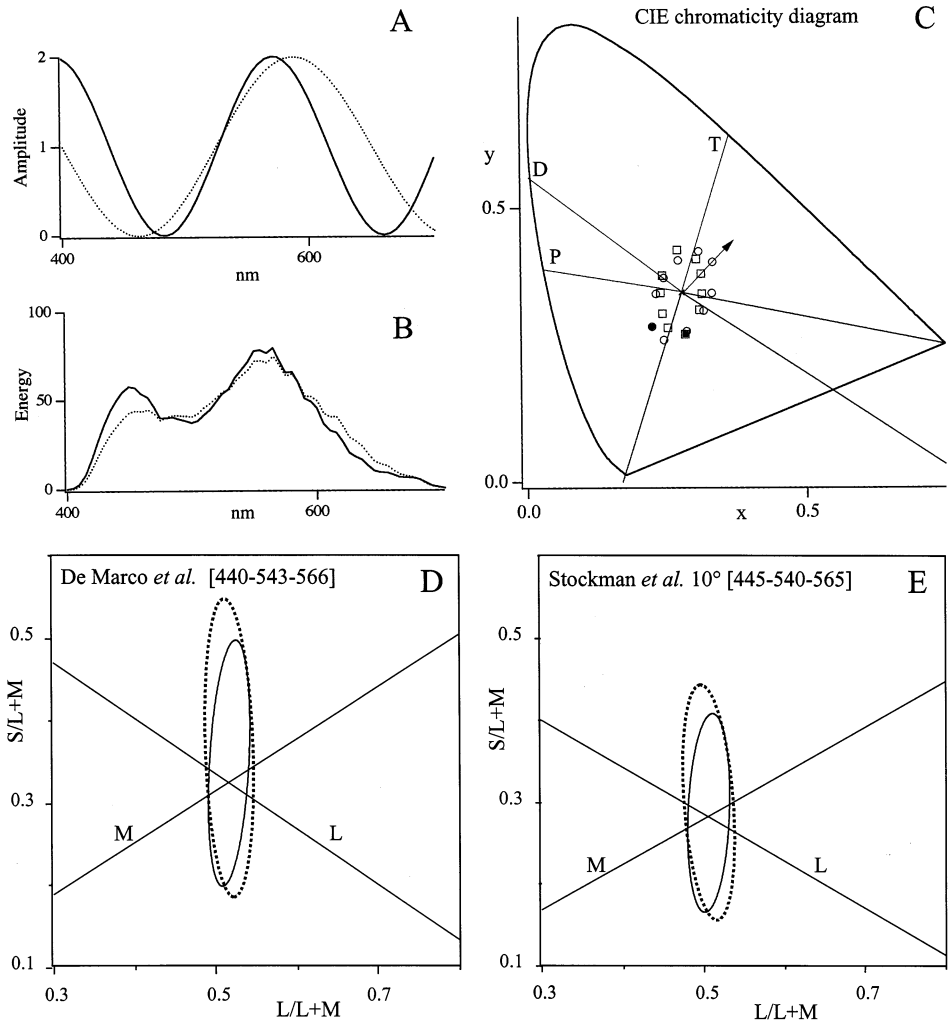

Fig. 2. (A) Profile of the electronic masks displayed by the LCD for 1.2 c with 180 deg (dashed line) and 1.7 c with 100 deg (continuous line) applied to the SPD of the light source. (B) Spectral power distributions (Eλ) measured after applying the two corresponding electronic masks. (C) The chromaticity co-ordinates of the two comb frequencies (circles: 1.2 c, squares: 1.7 c) for the ten different phases are plotted in the CIE chromaticity diagram. The filled symbols indicate the 0 deg phase. P, D and T correspond to the protanopic, deuteranopic and tritanopic confusion lines crossing at the locus of the un-modulated spectrum. As indicated by the arrow, the chromaticity co-ordinates of 1.2 c with 180 deg and 1.7 c with 100 deg are located in the same direction of the diagram. (D) Chromaticity co-ordinates computed in the MacLeod–Boynton chromaticity diagram using De Marco et al. fundamentals and E: with Stockman et al. 10 deg fundamentals. The elliptical contours instead of the data points are plotted in the diagrams. The axes correspond to the L and S-cone fundamentals normalised by the sum L + M. The M and L lines correspond to the M-cone and L-cone excitation lines.

matching functions as modified by Judd (1951), the DeMarco et al. fundamentals (DeMarco, Pokorny, & Smith, 1992), and the Stockman et al. 2 deg fundamentals (Stockman, MacLeod, & Johnson, 1993). In the large field condition, chromaticity coordinates were computed using the Stockman et al. 10 deg fundamentals (Stockman et al., 1993), which are based on the Stiles–Burch 2 deg fundamentals (Stiles & Burch, 1955). Chromaticity coordinates of 20 fully modulated comb-filtered spectra are plotted in the CIE chromaticity diagram in Fig. 2C. Chromaticity coordinates of the spectra were also plotted in the MacLeod–Boynton (MacLeod & Boynton, 1979) colour diagram using the DeMarco et al. fundamentals (Fig. 2D) and the Stockman et al. 10 deg fundamentals (Fig. 2E). For each observer, the spectral properties of the threshold stimuli were measured after the data were collected.

2.4. Observers

The four deuteranomalous observers (BR, CS, AWH and AH) were all male students in their first or second year of University who volunteered to participate in the experiment. Each had normal or corrected to normal acuity. Their colour vision was assessed using both Ishihara plates and a Nagel anomaloscope (type II). The authors VB and EV, both with normal trichromatic colour vision, also served as observers in these experiments.

3. Results

Colour discrimination thresholds were measured for ten different directions in the chromaticity diagram for each of two differing comb frequencies, in both large and small field conditions. For deuteranomalous observers, the spectral position of the anomalous M-cone fundamental was shifted towards the long-wavelengths in steps of one nanometer; chromaticity coordinates were computed for these different λ_{max} values. Each group of ten thresholds thus obtained was then fit by a procedure that determined the five parameters of the best-fitting ellipse (position x_0, y_0 of centre, orientation θ, and lengths a, b of the major and minor semi-axes, respectively). For each deuteranomalous observer, the spectral position of the anomalous M-cone fundamental that leads to the most similar best-fit ellipse's parameters was determined. For normal trichromat observers, fundamentals for the standard observer only were used (see Table 1 for parameters values).

3.1. Small field condition

When discrimination thresholds in the small field condition are plotted in the CIE chromaticity diagram, the two discrimination ellipses for VB (normal trichro-

Table 1
Best-fitted discrimination ellipse's parameters

Observers	Comb frequency	x	y	Length	a/b	size $\times 10^3$	θ	ρ
2 deg field								
CIE								
BR	1.2	0.2764	0.35	0.488	1.78	1.50	142.6	0.949
	1.7	0.2816	0.3489	0.056	2.09	1.18	146.3	0.977
VB	1.2	0.2762	0.3358	0.0284	2.58	0.25	71.3	0.985
	1.7	0.2796	0.3427	0.028	2.55	0.24	68.6	0.989
DeMarco et al. [440–540–566]								
BR	1.2	0.5135	0.3036	0.055	2.22	1.07	85.0	0.960
	1.7	0.5187	0.3028	0.0546	1.80	1.30	75.8	0.926
VB	1.2	0.516	0.332	0.057	8.38	0.30	90.3	0.999
	1.7	0.5168	0.3157	0.0532	7.82	0.28	91.0	0.999
DeMarco et al. [440–559–566]								
BR	1.2	0.4989	0.2948	0.054	9.00	0.25	90.2	0.999
	1.7	0.4986	0.2965	0.0544	8.77	0.26	91.7	0.999
8.5 deg annulus								
Stockman et al. 10 deg [445–540–565]								
CS	1.2	0.5075	0.2345	0.0248	1.94	0.25	85.6	0.925
	1.7	0.5073	0.2374	0.022	1.34	0.28	111.4	0.777
AWH	1.2	0.5063	0.2378	0.0442	1.73	0.89	47.8	0.948
	1.7	0.5109	0.2395	0.0494	1.67	1.15	30.9	0.896
AH	1.2	0.5078	0.237	0.0368	1.52	0.70	42.8	0.749
	1.7	0.5138	0.2404	0.0386	1.21	0.97	31.0	0.317
EV	1.2	0.5084	0.2377	0.0194	5.71	0.05	90.9	0.998
	1.7	0.5084	0.2377	0.0172	4.53	0.05	89.1	0.998
Stockman et al. 10 deg [445–559–565]								
CS	1.2	0.4922	0.2276	0.0246	8.79	0.05	90.4	0.999
	1.7	0.492	0.2306	0.0234	8.36	0.05	92.1	0.998
Stockman et al. 10 deg [445–561–565]								
AWH	1.2	0.4949	0.2325	0.0324	6.75	0.12	90.7	0.996
	1.7	0.4954	0.2317	0.037	8.04	0.13	90.7	0.995
AH	1.2	0.4954	0.2307	0.0318	7.95	0.10	91.3	0.998
	1.7	0.4956	0.2348	0.348	8.29	0.11	90.0	0.933
Comparison 2 vs. 8.5 deg for observer VB								
Stockman et al. 2 deg [445–540–570]								
	1.2	0.514	0.2971	0.0512	7.53	0.27	90.6	0.999
	1.7	0.5148	0.288	0.0456	6.51	0.25	91.8	0.999
Stockman et al. 10 deg [445–540–565]								
	1.2	0.5046	0.2757	0.0378	5.56	0.20	98.5	0.999
	1.7	0.5051	0.2766	0.0383	5.10	0.23	98.3	0.998

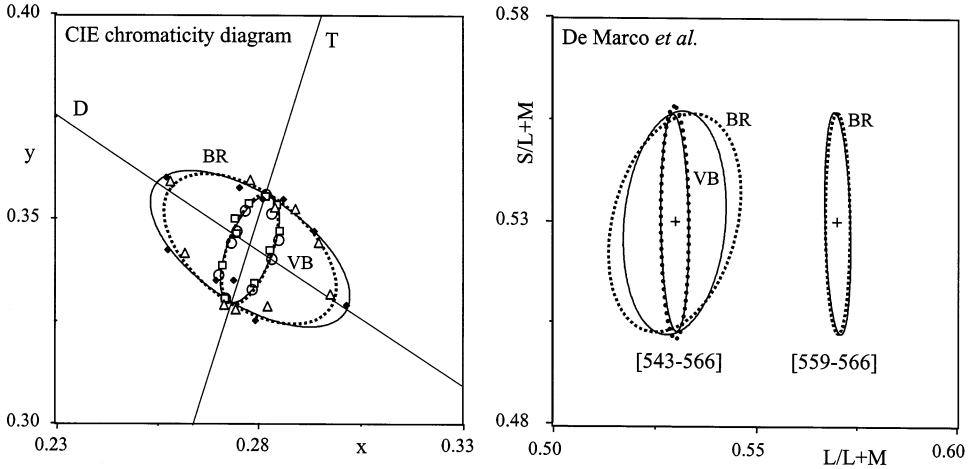

Fig. 3. Left: Discrimination thresholds (1.2 c: diamonds; 1.7 c: triangles) for BR (deuteranomalous) and for VB (normal trichromat) (1.2 c: squares; 1.7 c: circles) are plotted in the CIE chromaticity diagram. Eliptical contours are fitted to each set of data (1.2 c dashed lines; 1.7 c: continuous lines). Note that a single ellipse fits VB's results but not BR's. D and T correspond respectively to the deuteranopic and tritanopic confusion lines crossing at the locus of the unmodulated spectrum. Right: Computed chromaticity co-ordinates for these results are plotted for BR and VB in a MacLeod–Boynton diagram using the DeMarco et al. with a standard spectral position of the M-cone fundamental of 543 nm (left) and a deuteranomalous position of 559 nm for BR (right). For clarity, the best-fitted ellipses only are plotted; they are plotted on the same chart for purposes of comparison. As indicated in Table 1, there are small variations in the centre of the ellipses, thus when plotted on the same chart, the scale is respected but not the exact location.

mat) have similar size and are oriented approximately along the tritanopic confusion line (Fig. 3, left panel). The ellipses of BR (deuteranomalous) have different sizes and both are oriented along the deuteranopic confusion line. When plotted in a MacLeod–Boynton diagram, VB's discrimination ellipses are of similar size and vertically oriented, while BR's ellipses vary in size and orientation and are slightly tilted to the right (Fig. 3, right panel, on the left). The difference between BR's two ellipses is minimised for an anomalous M-cone fundamental with λ_{max} equals to 559 nm. When this anomalous cone fundamental is used, BR's two ellipses lie nearly atop one another with a vertical orientation and a size similar to that of VB (Fig. 3, right panel, on the right).

3.2. Large field condition

Fig. 4 shows discrimination thresholds of the four observers for frequencies 1.2 c (Fig. 4A) and 1.7 c (Fig. 4B). As classically reported, discrimination ellipses vary noticeably among deuteranomalous observers (Regan et al., 1994). AH and AWH's discrimination ellipses are oriented roughly along the M-cone excitation line (although in case of AH, validity of the parameters should be regarded cautiously considering the low value of the goodness of fit). For the three deuteranomalous observers, the discrimination ellipses vary in size and orientation with comb frequency, whereas for the normal trichromat EV, the two ellipses are oriented vertically and are of about the same size. As was found with BR, shifting the M-cone fundamental towards the long-wavelength end of the spectrum causes the plotted ellipses to take on a vertical orientation. The discrimination ellipses of all four observers in the large field condition are plotted together in Fig. 4C, using the optimal anomalous fundamentals (with λ_{max} of 561 nm for AWH and AH; and of 559 nm for CS). The size of CS' ellipses is comparable to that of EV's, while those of AH and AWH are about two to three times as large.

3.3. Comparison between conditions

Fig. 5 shows VB's discrimination ellipses for the small and large field conditions plotted together. The ellipses obtained in the small field conditions are plotted in the MacLeod–Boynton diagram using the DeMarco et al. and the Stockman et al. 2 deg fundamentals, while those for the large field conditions are plotted using the Stockman et al. 10 deg fundamentals. Discrimination ellipses obtained using the former two fundamentals are more elongated than those obtained using the last fundamentals, which are smaller and are tilted slightly leftwards.

4. Discussion

We succeeded in finding the spectral position of the anomalous cone fundamental that minimises the difference between the discrimination ellipses found for each deuteranomalous observer. It is the close alignment of the members of each pair of ellipses that indicates a correct choice of cone fundamentals. The alignment

depends on the use of metameric comb-filtered spectra at the two chosen comb frequencies, and the metamerism depends, in turn, on the choice of fundamentals. In the MacLeod–Boynton diagram, the aligned ellipses of the deuteranomalous observers are oriented vertically, as was also found to be true of the ellipses for the normal trichromats. The vertical orientation indicates a greater sensitivity to L-axis modulations than to S-axis modulations in this colour space (Romero, Garcia, Jinenez del Barco, & Hitza, 1993) and is believed to be the consequence of the correct choice of the fundamentals.

Owing to the large overlap with the normal cone fundamental, the psychophysical determination of the spectral sensitivity of the anomalous cone fundamental has been difficult to perform in anomalous trichromats. Recently, Sharpe et al. (1998) measured the spectral sensitivity curves of the anomalous fundamentals retained by dichromats (protanopes, or more conveniently named by the authors 'anomalous protanopes') and that are shared with anomalous trichromates (protanomalous) observers. Since there are no such 'anomalous deuteranopes' (deuteranopes retain the normal L-cone fundamental and not the anomalous M-cone fundamental), spectral sensitivity for these fundamentals remains to be determined. DeMarco et al. (1992), proposed fundamentals for a 'standard deuteranomalous observer' with a spectral separation of 6 nm between the anomalous M- and the normal L-cone fundamental (560–566 nm). With a spectral separation of 7 nm (559–566 nm), DeMarco et al. fundamentals provide a suitable chromaticity diagram to represent BR's performance. However, there is evidence from molecular biology studies (Merbs & Nathans, 1992; Ansejo, Rim, & Oprian, 1994) indicating that deuteranomalous observers do not all share the same anoma-

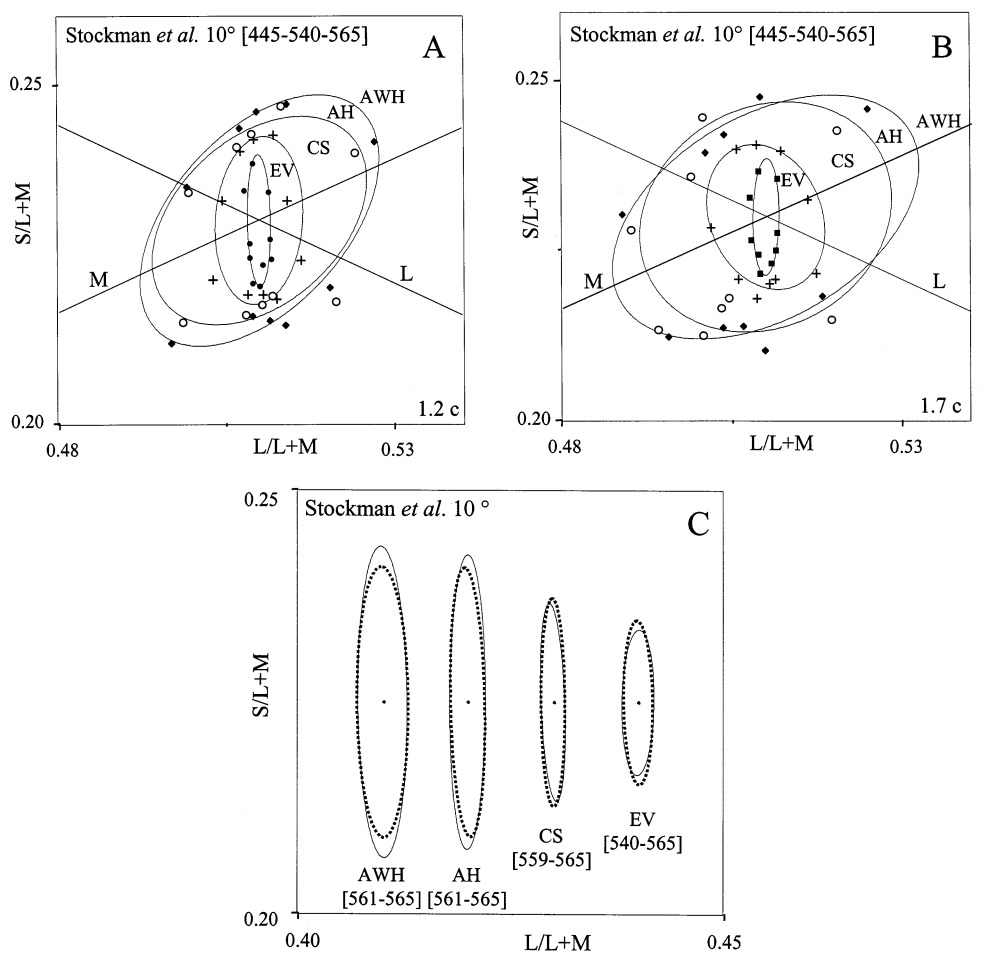

Fig. 4. (A) and (B) Discrimination thresholds for three deuteranomalous CS (crosses), AH (empty circles) AWH (diamonds) and one normal EV (filled circles) observers, are plotted in a MacLeod–Boynton diagram using standard Stockman et al. 10 deg fundamentals. Panel A shows results for comb frequency 1.2 c, panel B for 1.7 c. The best fitted-ellipse contour to the set of thresholds for each frequency is also plotted. (C) The chromaticity co-ordinates were computed with the spectral position of the M-cone fundamental as indicated in brackets by the first number; the second number corresponding to the unchanged spectral position of the standard L-cone fundamental (565 nm). The M-cone fundamental position is 561 nm for AWH and AH and 559 nm for CS. For comparison, the best-fitted ellipses for the two comb frequencies of all deuteranomalous observers are plotted together with EV's best-fitted ellipses (normal trichromat) on the same chart.

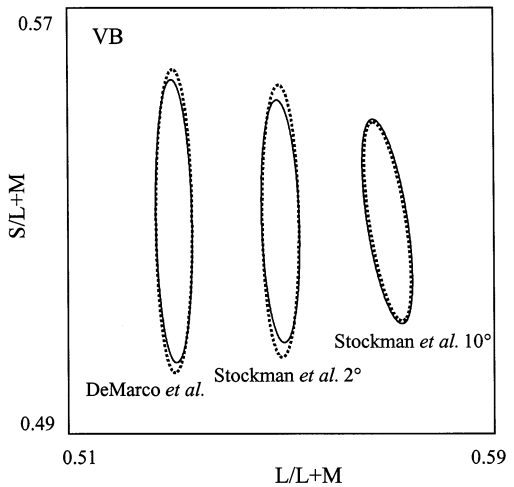

Fig. 5. Chromaticity co-ordinates of discrimination thresholds for colour normal observer VB are computed in a MacLeod–Boynton diagram using the DeMarco et al. and Stockman et al. 2 deg fundamentals and Stockman et al. 10 deg fundamentals for small field and large field conditions respectively. The best-fitted ellipses only are presented and re-plotted on the same chart for comparison.

lous pigment. X-linked pigment genes produce families of hybrid pigments (combinations of M and L pigments), and a monotonic relationship exists between the maximum of the pigment absorption curve (λ_{max}) and the fraction of the hybrid pigment derived from the L and M-cone pigments (Sharpe et al., 1998). In vitro studies (Merbs & Nathans, 1992; Asenjo et al., 1994), using recombinant pigments produced in tissue culture cells, show a spectral separation between the hybrid and normal pigment of 4–12 nm depending on the fraction from which the hybrid pigment is derived. The determination of the λ_{max} we made of the anomalous M-cone fundamental for each individual deuteranomalous observers shows a 4–7 nm differences in the spectral separation between the two fundamentals, suggesting difference in cone-fundamentals among our observers. Also relevant in the choice of fundamental for deuteranomalous and not taken into account in this study, is the existence of a common dimorphism of the normal L-fundamental giving rise of two L-cone fundamentals differing in their spectral position. DeMarco et al. and Stockman et al. use a L-cone fundamental whose sensitivity is intermediate between the two common variants.

There is also variation among the anomalous observers in the absolute level of discrimination, as indicated by variation of 2.8-fold in ellipse size, which agrees with the variation of two- to three-fold found among normal trichromats (Romero et al., 1993). This agreement suggests that when the spectral position of the anomalous cone fundamental is taken into account, the range of variation in colour discrimination is comparable to that of normal trichromats (Pokorny & Smith, 1977).

Comparison of results from small and large field conditions for observer VB indicates than when field size increases, the size of colour discrimination ellipses decreases (e.g. Brown, 1952; Yebra et al., 1994). The decrease, shown in Fig. 5, is due mainly to a reduction in vertical semi-axis length, again in agreement with the results of Yebra and colleagues. This reduction corresponds to an increase in sensitivity to modulations along the S direction, and may be due to a higher density of S-cones at the retinal eccentricities stimulated by the large field stimulus, although rod intrusion cannot be ruled out at the relatively low luminance levels used in these experiments. VB's discrimination ellipses are also tilted slightly to the left of vertical. This may be due to the effect of biological variables like macular pigment density, lens thickness, photoreceptor optical density and spectral position of photoreceptors that cause transformation of colorimetric axes (Smith & Pokorny, 1995) and that were not taken into account in this study.

Our object was to represent discrimination performance of anomalous observers in a suitable chromaticity diagram where the spectral position of the anomalous cone fundamental is taken into account. The technique presented here shows that comb-filtered spectra can take into account this and pre-photoreceptoral causes of variation in observer spectral sensitivity.

Acknowledgements

The authors wish to thank Horace Barlow and Javier Romero for their support and advices. We are also very thankful to an anonymous referee whose review greatly improved both the text and the presentation of this paper. This work was done while Valérie Bonnardel was supported by a MRC Grant (23 087-PUA-R35), and Éva Valero by a Travel Grant from Conserjería de Educación y Ciencia de la Junta de Andalucía.

References

Asenjo, A. B., Rim, J., & Oprian, D. D. (1994). Molecular determinants of human red/green color discrimination. *Neuron*, *266*, 647–675.

Barlow, H. B. (1982). What causes trichromacy? A theoretical analysis using comb-filtered spectra. *Vision Research*, *22*, 635–643.

Bonnardel, V., Bellemare, H., & Mollon, J. D. (1996). Measurements of human sensitivity to comb-filtered spectra. *Vision Research*, *36*, 2713–2720.

Bonnardel, V., Ruderman, D. L., & Barlow, H. B. (1997). A fast determination of the Spectral Modulation Sensitivity Function: A comparison between trichromats and deuteranopes. In C. R. Cavonius, *Color vision deficiencies XIII* (pp. 415–424). Dordrecht: Kluver.

Bonnardel, V. (1998). Demonstration of a new stimulator for human colour vision testing. *Journal of Physiology London*, *506*, 31.

Brill, M. H., & Benzschawel, T. (1985). Remarks on signal-processing explanations of the trichromacy of vision. *Journal of the Optical Society of America*, *A*, *2*, 1794–1796.

Brown, W. R. J. (1952). The effect of field size and chromatic surrounding on color discrimination. *Journal of the Optical Society of America*, *42*, 837–844.

DeMarco, P., Pokorny, J., & Smith, V. C. (1992). Full-spectrum cone sensitivity functions for X-chromosome-linked anomalous trichromats. *Journal of Optical Society of America*, *A*, *9*, 1465–1476.

Judd, B.D. (1951). Report from the US Secretariat, Committee on Colorimetry and Artificial Daylight. Proc. CIE 1, part 7, p.11 (Stockholm). Paris Bureau Central CIE.

MacLeod, D. I. A., & Boynton, R. M. (1979). Chromaticity diagram showing cone excitation by stimuli of equal luminance. *Journal of Optical Society of America*, *69*, 1183–1186.

Merbs, S. L., & Nathans, J. (1992). Absorption spectra of the hybrid pigments responsible for anomalous color vision. *Science*, *258*, 464–466.

Pokorny, J., & Smith, V. C. (1977). Evaluation of single-pigment shift model of anomalous trichromacy. *Journal of Optical Society of America*, *67*, 1196–1209.

Regan, B. C., Reffin, J. P., & Mollon, J. D. (1994). Luminance noise and the rapid determination of discrimination ellipses in color deficiency. *Vision Research*, *34*, 24–44.

Romero, J., Garcia, J. A., Jimenez del Barco, L., & Hita, E. (1993). Evaluation of color-discrimination ellipsoids in two-color spaces. *Journal of the Optical Society of America*, *A*, *10*, 827–837.

Sharpe, L. T., Stockman, A., Jägle, H., Knau, H., Klaussen, G., Reitner, A., & Nathans, J. (1998). Red, green, and red-green hybrid pigments in the human retina: correlations between deduced protein sequences and psychophysically measured spectral sensitivities. *The Journal of Neuroscience*, *18*, 10053–10069.

Smith, V. C., & Pokorny, J. (1995). Chromatic-discrimination axes, CRT phosphor spectra, and individual variation in color vision. *Journal of Optical Society of America*, *A*, *12*, 27–35.

Stiles, W. S., & Burch, J. M. (1955). Interim report to the Commission Internationale de l'Eclairage Zurich, 1955, on the National Physical Laboratory's investigation of colour-matching. *Opt. Acta*, *2*, 168–181.

Stockman, A., MacLeod, D. I. A., & Johnson, N. E. (1993). Spectral sensitivities of the human cones. *Journal of the Optical Society of America*, *A*, *12*, 2491–2521.

Yebra, J., Garcia, J. A., & Romero, J. (1994). Color discrimination data for 2 and 8 deg and normalised ellipses. *Journal of Optics (Paris)*, *25*, 231–242.